European Journal of Medicinal Chemistry 83 (2014) 609–616

Contents lists available at ScienceDirect

European Journal of Medicinal Chemistry

journal homepage: http://www.elsevier.com/locate/ejmech

Original article

Pyridopyrimidinone inhibitors of HIV-1 RNase H

Emile J. Velthuisen*, Brian A. Johns, Peter Gerondelis, Yan Chen, Ming Li, Ke Mou, Wenwen Zhang, John W. Seal, Kendra E. Hightower, Sonia R. Miranda, Kevin Brown, Lisa Leesnitzer

GlaxoSmithKline Research & Development, Infectious Diseases Therapeutic Area Unit, Five Moore Drive, Research Triangle Park, NC 27709, United States

ARTICLE INFO

Article history:
Received 7 April 2014
Received in revised form
25 June 2014
Accepted 27 June 2014
Available online 28 June 2014

Keywords:
HIV
AIDS
Reverse transcriptase
Integrase
Two-metal binder
Endonuclease

ABSTRACT

Using a structure based pharmacophore design, a weak inhibitor of RNase H, identified from a small library of two metal binding HIV-1 integrase inhibitors, was optimized for potency and physicochemical properties. This manuscript describes the SAR and *in vivo* DMPK for the pyridopyrimidinone class of inhibitors.

1. Introduction

The human immunodeficiency virus type 1 (HIV-1) utilizes three virally-encoded enzymes to facilitate replication following infection of the host: reverse transcriptase, integrase and protease. Accordingly, these enzymes have become attractive targets for disrupting the viral lifecycle with antiretroviral drugs. However, despite over 30 approved agents and combination treatment options, HIV therapy remains problematic due to drug resistance and tolerability.

HIV reverse transcriptase (RT) is a heterodimeric protein responsible for conversion of single stranded viral RNA into double stranded DNA. This is accomplished through the concerted function of two active sites on the p66 domain; the N-terminus DNA polymerase and a separate ribonuclease H (RNase H) region located on the C-terminus. RNase H is a metal dependent endonuclease that hydrolyzes RNA as part of an RNA/DNA hybrid duplex. Several of these RNA nicking events take place during the reverse transcription process to facilitate template RNA dissociation and negative DNA strand transfer after the initial strong stop minus strand synthesis. Additionally, the RNase H activity facilitates the necessary selective cleavage to free up the polypurine tract (ppt) to act as a positive strand primer and is responsible for removal of the original tRNA primer. Mutation studies have demonstrated that RNase H is essential for viral replication, and despite the effort of numerous groups, the only approved drugs targeting RT are inhibitors of the polymerase function. While inhibitors of the RT polymerase function have enjoyed a rich history of successful research, inhibitors of the RNase H functional biochemistry have not. In fact, with the development of both HIV protease and integrase inhibitors, HIV RNase H has the dubious and unique distinction of being the only virally encoded enzymatic function that is not part of a chemotherapeutic intervention now a full 30 years into the HIV/AIDS epidemic.

High resolution crystallography of RNase H complexed to the RNA/DNA hybrid reveals two Mg^{2+} ions as essential in formation of the active catalytic complex. Interestingly, a very similar two-metal motif is required for the catalytic activity of strand-transfer integrase inhibitors, and indeed, it has been demonstrated that the two

Abbreviations: ADME, absorption, distribution, metabolism, excretion; AIDS, acquired immunodeficiency syndrome; Cl, clearance; CLND, chemi-luminescent nitrogen detection; DIPEA, diisopropyl ethyl amine; DMPK, drug metabolism and pharmacokinetics; DNAUC, dose-normalized area under the curve; F, oral bioavailability; HAART, highly active antiretroviral therapy; HIV, human immunodeficiency virus; IN, Integrase; INST, integrase strand transfer; PFI, property forecast index; RT, reverse transcriptase; RTST, reverse transcriptase strand transfer; TMS, trimethylsilyl.

* Corresponding author.
E-mail address: emile.j.velthuisen@gsk.com (E.J. Velthuisen).

http://dx.doi.org/10.1016/j.ejmech.2014.06.061
0223-5234/

enzymes share numerous structural features in their active sites [1]. Because of the similarity between these two targets, we initiated a screen of our two-metal binding library to identify novel inhibitors in an RT strand-transfer biochemical assay. Herein, we report the results of the screening effort and the design of highly selective and potent RNase H inhibitors. In addition, the pharmacokinetic profile for several of these compounds will be discussed.

2. Results and discussion

2.1. Focused metal-binder screen

As part of an effort to identify novel starting points for the development of selective inhibitors of HIV RNase H activity, a small library of two-metal chelating HIV integrase inhibitors (consisting of internal legacy examples as well as literature compounds) were screened for the ability to inhibit HIV RT strand transfer activity in a modified version of the assay described by Gabbara and Peliska [2]. Because this assay requires both RNase H and DNA polymerase activities of RT, hits were counter screened in secondary assays similar to those previously described to resolve specific inhibitors of RNase H from those that inhibited the DNA polymerase activity of RT [3,4]. This subset of compounds represents a larger collection of 2-metal binders with an emphasis upon scaffold diversity. The results of our screening identified several naphthyridine scaffolds as weak inhibitors of RT strand transfer which became the starting point for our optimization (Fig. 1).

2.2. Chemistry

In designing more potent and selective RNase H inhibitors, it is important to consider which structural features of the naphthyridine hits are part of the integrase strand transfer pharmacophore [5,6] and which features can be appended to the molecule to better mimic the reverse transcriptase strand transfer pharmacophore [7,8]. In general, integrase strand transfer inhibitors contain three domains: a hydrophobic region, a flexible linker, and a two-metal binding region [9]. As can be seen in Fig. 1, the 4-chloro benzylamine is crucial for the integrase strand transfer activity [5,10] (**2** $^{INST}IC_{50} = 0.135\ \mu M$; **3** $^{INST}IC_{50} = 11\ \mu M$) and removal of this group is likely beneficial for designing a more selective RT strand transfer inhibitor. In addition, the 5-amino substituent of naphthyridine **1** [11] appears to provide a slight boost in potency in the RT-ST assay (**1** $^{RTST}IC_{50} = 10\ \mu M$; **3** $^{RTST}IC_{50} = 11\ \mu M$) and could serve as a useful functional handle for future SAR exploration. There have been numerous examples reported in the literature of *N*-hydroxyimides as potent endonuclease inhibitors [12]. Our interest in this scaffold was to take a well established two-metal binding motif (i.e. **4**) and incorporate this onto naphthyridine **3** (Fig. 2). Although the oxygen of the carbonyl imide of **4** is likely better match for the hard metal properties of the divalent magnesium cofactor [13], the synthetic accessibility of a pyridopyrimidinone such as **5** made this a very attractive scaffold to initially investigate. In addition, during the course of our studies, an *N*-hydroxy naphthyridinone inhibitor of RNase H was reported, further fueling our interest in this architecture [14,15].

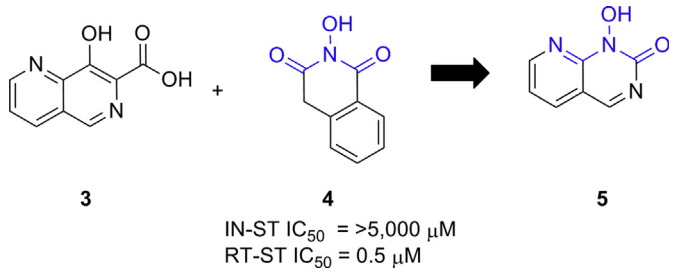

Fig. 2. Incorporating the two-metal binding motif of a known RNase H inhibitor.

The synthesis of 5-amino substituted pyridopyrimidinone analogs is shown in Scheme 1. Two slightly different protecting group strategies were utilized in the synthesis of these analogs and both are described. Starting from commercially available 2-fluoronicotinic acid, nucleophilic addition of *O*-benzyl hydroxylamine under microwave irradiation conditions provided pyridine **7**. The carboxylic acid was then esterified using TMS-diazomethane and the *O*-benzyl hydroxylamine moiety was acylated with 4-methoxybenzylisocyanate. Cyclization to form the imide was achieved using sodium methoxide and the 4-methyoxybenzyl group was then oxidatively cleaved using ceric ammonium nitrate. In a similar manner, synthesis of the *tert*-butyl protected analogs started with addition of *O*-*tert*-butyl hydroxylamine into 2-fluoronicotinonitrile **10**. The nitrile was hydrolyzed under basic conditions and the resulting carboxylic acid was esterified using TMS-diazomethane. Aniline **11** was treated with trichloroacetyl isocyanate and the resulting urea **12** was then cyclized and concomitantly deprotected using sodium methoxide. Treatment of the imide **9** or **13** with phosphorous oxychloride afforded chloride **14** or **15** which underwent nucleophilic addition with a variety of amines. The protecting group was then removed under acidic conditions to afford examples **18**–**29** (Table 1).

2.3. Structure activity relationship

To establish whether these compounds conveyed an antiviral effect, a single round of infection assay was used as previously described [16]. This assay has been employed to resolve antiviral activity for separate NNRTI and integrase inhibitor development programs and has been engineered to allow for the mechanistic resolution of susceptibility changes against site-directed mutants specific for these types of inhibitors. All of the compounds reported in Table 1 were tested for activity against RT-polymerase but

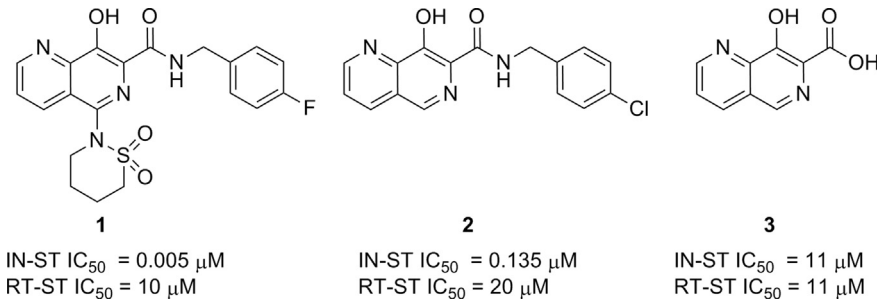

Fig. 1. Initial hits from a RT strand transfer screen.

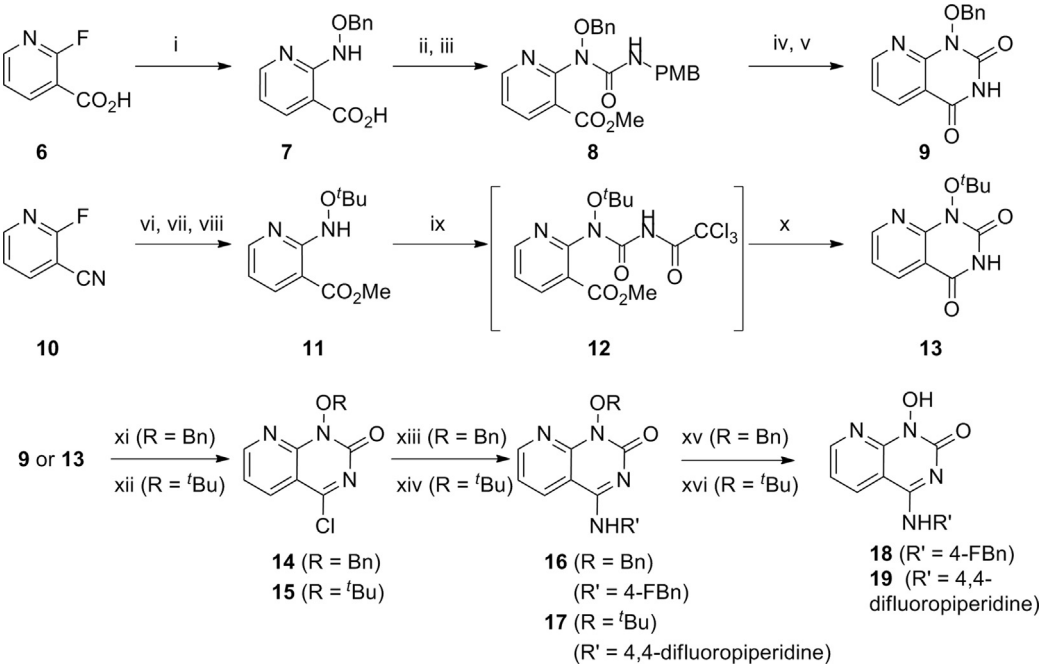

Scheme 1. Synthesis of pyridopyrimidinone analogs. Reagents and conditions: (i) NH_2OBn, DIPEA (69%); (ii) TMS-CH_2N_2, Et_2O (96%); (iii) 1-isocyanatomethyl-4-methoxybenzene, 1,2-DCE (73%); (iv) NaOMe, MeOH (74%); (v) cerium (IV) ammonium nitrate, CH_3CN/H_2O (79%); (vi) $NH_2O^tBu \cdot HCl$, DIPEA (96%); (vii) NaOH, H_2O (79%); (viii) TMS-CH_2N_2, Et_2O (97%); (ix) trichloroacetyl isocyanate, 1,2-DCE; (x) NaOMe, MeOH (75% over 2-steps); (xi) $POCl_3$, DIPEA (97%); (xii) $POCl_3$, DIPEA (97%); (xiii) 4-fluorobenzyl amine, DMF (85%); (xiv) 4,4-difluoropiperidine, DIPEA, DMF (81%); (xv) HBr, AcOH, 80 °C; (xvi) TFA, DCM (65%).

demonstrated no inhibition up to a concentration of 10 μM. Dose-dependent cytotoxicity measures were determined in parallel with the antiviral measures by the use of cells that were pre-infected and constitutively express the fire-fly luciferase reporter. Since the virus employed to create these cells is replication defective, inhibition of this signal would reflect a mechanism that is independent of viral reverse transcription and integration and hence resolve a correlate (CC_{50}) for the resolution of selectivity versus the antiviral effect (IC_{50}). In addition to optimization of antiviral potency, the optimization of physicochemical properties was also taken into account. There have been numerous studies in the literature that demonstrate a negative impact upon compound developability with an increasing number of aromatic rings and high lipophilicity [17,18]. A simple metric to track this is known as the property forecast index (PFI) which is the sum of the chromatographic log $D_{pH7.4}$ plus the aromatic ring count [19]. A recent retrospective analysis indicates that 75% of orally available marketed drugs have a PFI of ≤6 [20]. To measure some of the developability criteria for analogs synthesized, both the permeability and solubility for select compounds are reported (Table 2).

As a starting point for our optimization, 4-fluorobenzyl amine **18** was synthesized. This analog had modest potency in the single round infectivity assay ($^{PHIV}IC_{50}$ = 0.50 μM) and decent potency in the RNase H biochemical assay ($^{RTST}IC_{50}$ = 0.158 μM). In addition, this analog was weakly active in the IN-strand transfer assay ($^{INST}IC_{50}$ = 3.16 μM) and did not exhibit any cytotoxicity up to a maximum concentration of 39 μM. Although a promising lead in terms of potency and selectivity for RNase H over INST activity, the PFI (=7.2) for this compound was higher than desired. Unfortunately, removal of the 4-fluorobenzyl amine and installation of non-aromatic containing side chains (i.e. **19** and **20**) had a deleterious effect upon both the antiviral (**19** $^{PHIV}IC_{50}$ = 1.91 μM; **20** $^{PHIV}IC_{50}$ = 0.71 μM) and the RNase H activity (**19** $^{RTST}IC_{50}$ = 0.501 μM; **20** $^{RTST}IC_{50}$ = 0.398 μM) although it did offer lower PFI values (**19** = 6.3; **20** = 2.6).

To explore the antiviral effect of additional aromatic groups appended to the lead **18**, biphenyl aniline **21** was synthesized. This analog was significantly more potent than **18** in both the antiviral ($^{PHIV}IC_{50}$ = 0.10 μM) and biochemical RNase H assay ($^{RTST}IC_{50}$ = 0.032 μM). Interestingly, there was also modest activity in the IN strand transfer assay ($^{INST}IC_{50}$ = 0.6 μM) and measurable cellular cytotoxicity at a concentration of 2.5 μM. Installation of biphenyl benzyl amine **22** afforded a similar antiviral profile as biphenyl aniline **21,** albeit less potent in the single round infectivity assay ($^{PHIV}IC_{50}$ = 0.20 μM) and significantly more potent in the RNase H assay ($^{RTST}IC_{50}$ = 0.010 μM). As with the biphenyl analog, there was measurable activity in the IN strand transfer assay ($^{INST}IC_{50}$ = 0.8 μM) and slightly less cytotoxicity (CC_{50} = 4 μM).

In designing analogs that improve the physicochemical properties of this series, an emphasis was placed upon incorporation of heteroaromatic and heterocyclic groups. An example of this is replacement of the distal phenyl ring of **21** with a pyridine such as in compound **23**. Although this initial analog was less potent in both biochemical assays ($^{RTST}IC_{50}$ = 0.079 μM; $^{INST}IC_{50}$ = 0.4 μM) and the single round infectivity assay ($^{PHIV}IC_{50}$ = 0.26 μM), there was no measurable cytotoxicity up to a maximum concentration of 50 μM, and the PFI was significantly lower, as expected (=5). Interestingly, the benzyl amine version of this analog (**24**) was nearly equipotent in the antiviral assay ($^{PHIV}IC_{50}$ = 0.30 μM) albeit more potent in the RNase H biochemical assay ($^{RTST}IC_{50}$ = 0.016 μM) and similar in potency in the IN strand transfer activity ($^{INST}IC_{50}$ = 1.26 μM).

To further improve upon the physicochemical properties of this series, we investigated replacement of the distal aromatic ring of **21** with morpholine. The 4-morpholino phenyl analog **25** was slightly less potent than biphenyl **21** in the antiviral assay ($^{PHIV}IC_{50}$ = 0.25 μM), however it had similar potency in both biochemical assays ($^{RTST}IC_{50}$ = 0.050 μM; $^{INST}IC_{50}$ = 0.5 μM). As expected, the PFI of this compound (=4) was significantly lower than the corresponding biphenyl analog **21** (PFI = 7.2).

Table 1
Antiviral profile of pyridopyrimidinone analogs.

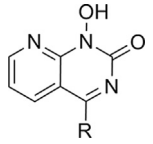

Cmpd	Structure	pHIV IC_{50} (μM)	RT-RNase H IC_{50} (μM)	IN-ST IC_{50} (μM)	Fold selectivity RT/IN-ST	Cytotoxicity CC_{50} (μM)	PFI
18	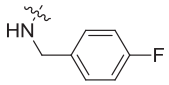	0.50	0.158	3.16	20	>39	7.2
19	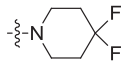	1.91	0.501	7.94	16	>50	6.3
20	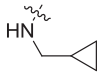	0.71	0.398	3.9	10	>39	2.6
21	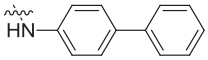	0.10	0.032	0.79	25	2.5	7.2
22	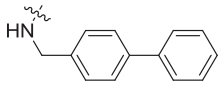	0.20	0.010	0.63	63	4.0	7.0
23	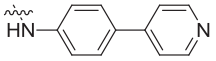	0.26	0.079	1.99	25	>50	5.0
24	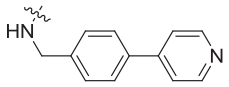	0.30	0.016	1.26	78	>50	5
25	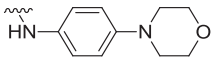	0.25	0.050	0.50	10	>50	4
26	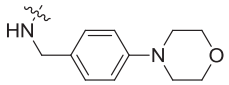	0.47	0.100	1.58	16	>50	5
27	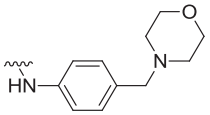	0.16	0.200	1.3	7	>50	3.6
28	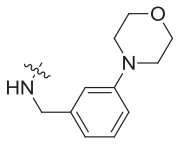	0.38	0.200	1.99	10	>30	4.4
29	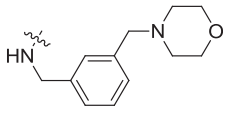	0.30	0.398	15.9	40	>50	6.5

Having identified a suitable replacement for the distal phenyl ring of **21**, our attention turned to optimizing the positioning of the morpholine group. The objective was to increase the antiviral potency of these compounds while maintaining a good selectivity of RNase H over IN strand transfer. The benzyl amine analog **26** did improve the desired selectivity in the biochemical assays (**25**, 10×; **26**; 16×) albeit at the cost of antiviral potency (**25**, $^{PHIV}IC_{50} = 0.25$ μM; **26**, $^{PHIV}IC_{50} = 0.47$ μM). Interestingly, synthesis of the 4-(morpholinomethyl)aniline **27**, where the extra methylene linker is now connected to the morpholine, provided an analog with increased potency in the antiviral ($^{PHIV}IC_{50} = 0.16$ μM) and IN strand transfer assays ($^{INST}IC_{50} = 1.3$ μM), although the activity in

Table 2
In vivo and developability profiles of pyridopyrimidinone analogs.

Cmpd	Cl (mL/min/kg)	$t_{1/2}$ (h)	i.v. DNAUC (ng h/mL/mg)	*F* (%)	Permeability (nm/s)	CLND (μM solubility)
21	5.9	7.4	2934	0	172	3
23	12	10	1942	0	13	3
24	16	0.5	1000	ND	16	16
25	45	2.4	314	ND	7	161
26	55	4.5	713	ND	14	293
27	70	0.4	226	ND	5	503

the RNase H biochemical assay was now slightly decreased ($^{RTST}IC_{50} = 0.200$ μM). Moving the distal morpholine from a para to meta position (**26**–**28**), also slightly improved the antiviral potency ($^{PHIV}IC_{50} = 0.38$ μM) while decreasing the inhibitory effect in both biochemical assays ($^{RTST}IC_{50} = 0.200$ μM; $^{INST}IC_{50} = 1.99$ μM). And finally, placing an extra methylene spacer between the phenyl ring and the morpholine (**29**) greatly reduced the IN-strand transfer activity ($^{INST}IC_{50} = 15.9$ μM) while further improving the antiviral potency ($^{PHIV}IC_{50} = 0.30$ μM).

During the course of our optimization, it became challenging to correlate closely between the antiviral and biochemical assays. One factor believed to contribute to this was poor cell permeability. As can be seen in Table 2, compound **21** has moderate cell permeability (172 nm/s), and there is a good correlation between the biochemical and antiviral assays (Table 1). However, many of the other analogs have low cell permeability (MDCK <16 nm/s) and also lack a reliable correlation between the antiviral and biochemical assays. Additional mechanism of action studies around these inhibitors will be published in due course.

2.4. In vivo DMPK

To evaluate metabolic stability, a number of analogs were dosed both intravenously and orally in Sprague–Dawley rats. In general, incorporation of the morpholine moiety (Table 2; **25**, **26**, **27**) resulted in higher clearance values relative to the hepatic blood flow in rats. Examples with distal aromatic or heteroaromatic groups (Table 2; **21**, **23**, **24**) had lower clearance values but no oral exposure was observed. Despite a modest permeability for **21**, poor solubility is likely limiting the oral absorption for this compound. Although the solubility for the more hydrophilic analogs (i.e. **25**, **26**, **27**) was greatly improved, both low permeability and high clearance values prevented progression of these compounds.

3. Conclusion

In conclusion, a number of HIV-1 RT RNase H inhibitors were synthesized. These compounds had good potency in the RNase H biochemical assay, were highly selective over HIV-1 RT polymerase, and were partially selectivity over HIV-1 Integrase. In addition to potency, the physicochemical properties of these compounds were optimized using the property forecast index (PFI). Because of this, several analogs had both improved solubility and good potency in the biochemical assay. Unfortunately, one of the challenges for this class of molecule was low permeability that resulted in poor *in vivo* oral absorption. Additionally, high clearance was observed when dosed intravenously in rats, possibly due to conjugation of the central hydroxamic acid moiety as a sulfate or glucuronide. Nonetheless, the ability to differentiate between two-metal utilizing endonuclease active sites through our initial structural modifications and demonstrate clear biochemical inhibition was very encouraging. This report focused on our attempts to design selective inhibitors of RNase H biochemistry over integrase. The alternative approach would be to build-in potency for both enzyme functions in a single molecule. Our efforts in this area resulting in highly potent dual inhibitors, as well as details on the mechanism of action, will be the subject of future publications.

4. Experimental section

4.1. Chemistry

All commercially available reagents were used without further purification. Column chromatography was carried out on silica gel (70–230 mesh). TLC was conducted on silica gel 250 micron, F254 plates. ^{1}H NMR spectra were recorded at 300 or 400 MHz. Melting points are uncorrected. Purities of test compounds were established by analytical HPLC (C-18 column, 5.0 micron, 0 → 100% CH_3CN (or MeOH)/water with 0.05–0.1% HCOOH (or TFA)) and UV detection with or without mass spectrometer detection. All test compounds showed >95% purity (AUCs by UV detection).

4.1.1. Procedure A (OBn protecting group)

*4.1.1.1. 2-{[(Phenylmethyl)oxy]amino}-3-pyridinecarboxylic acid (**7**).* A solution of 2-fluoro-3-pyridinecarboxylic acid (3.0 g, 21.2 mmol), *O*-(phenylmethyl)hydroxylamine (3.4 g, 27.6 mmol) and diisopropylethylamine (7.4 mL, 42.5 mmol) was irradiated in the microwave at 120 °C. After 40 min, the reaction mixture was concentrated *in vacuo* and the residue purified by silica gel chromatography (0–10% MeOH–dichloromethane) to afford the title compound (3.58 g, 69%) as a yellow solid: ^{1}H NMR (400 MHz, DMSO-d_6) δ ppm 8.26 (br. s., 1H), 8.07 (dd, *J* = 7.62, 1.37 Hz, 1H), 7.42–7.50 (m, 2H), 7.28–7.44 (m, 3H), 6.66–6.85 (m, 1H), 4.99 (s, 2H).

4.1.1.2. Methyl 2-{[(phenylmethyl)oxy]amino}-3-pyridinecarboxylate. A solution of 2-{[(phenylmethyl)oxy]amino}-3-pyridinecarboxylic acid (3.6 g, 14.7 mmol) in diethyl ether (37 mL) and methanol (37 mL) was treated with TMS-diazomethane (14.66 mL, 29.3 mmol, 2.0 M in hexane). After 5 min, AcOH was added dropwise until gas evolution ceased. The reaction mixture was concentrated *in vacuo* to afford the title compound (3.6 g, 96%) as an orange oil: ^{1}H NMR (400 MHz, CHLOROFORM-d) δ ppm 10.04 (s, 1H), 8.51 (dd, *J* = 1.8, 4.8 Hz, 1H), 8.17 (dd, *J* = 1.9, 7.8 Hz, 1H), 7.52–7.47 (m, 2H), 7.44–7.33 (m, 3H), 6.81 (dd, *J* = 4.8, 7.7 Hz, 1H), 5.09 (s, 2H), 3.85 (s, 3H); ES + MS: *m*/*z* = 259 (M+1).

*4.1.1.3. Methyl 2-{[({[4-(methyloxy)phenyl]methyl}amino)carbonyl][(phenylmethyl)oxy]amino}-3-pyridinecarboxylate (**8**).* A solution of methyl 2-{[(phenylmethyl)oxy]amino}-3-pyridinecarboxylate (3.1 g, 12 mmol) and 1-(isocyanatomethyl)-4-(methyloxy)benzene (5.1 mL, 36 mmol) in 1,2-dichloroethane (24 mL) was irradiated in microwave at 120 °C. After 90 min, the reaction mixture was concentrated *in vacuo* and the residue purified by silica gel chromatography (0–100% ethyl acetate–hexanes) to afford the title compound (3.7 g, 73%) as a white solid: ^{1}H NMR (400 MHz, CHLOROFORM-*d*) δ ppm 8.58 (dd, *J* = 4.88, 1.76 Hz, 1H), 8.10 (dd, *J* = 7.80, 1.76 Hz, 1H), 7.37–7.45 (m, 2H), 7.27–7.33 (m, 3H), 7.18–7.24 (m, 1H), 7.06 (d, *J* = 8.59 Hz, 2H), 6.76–6.89 (m, 2H), 4.95–5.04 (m, 2H), 4.26 (d, *J* = 5.85 Hz, 2H), 3.73–3.81 (m, 6H); ES + MS: *m*/*z* = 422 (M+1).

*4.1.1.4. 1-[(Phenylmethyl)oxy]pyrido[2,3-d]pyrimidine-2,4(1H, 3H)-dione (**9**).* An ice-cold solution of methyl 2-{[({[4-(methyloxy)phenyl]methyl}amino)carbonyl][(phenylmethyl)oxy]amino}-3-pyridinecarboxylate (1.0 g, 2.49 mmol) in methanol (25 mL) was treated with sodium methoxide (0.062 mL, 0.249 mmol, 25% in MeOH). After 5 min, the white precipitate was filtered and washed

with MeOH to afford the title compound (0.72 g, 74%): ^{1}H NMR (400 MHz, DMSO-d_6) δ ppm 8.74–8.92 (m, 1H), 8.33–8.53 (m, 1H), 7.59–7.65 (m, 2H), 7.42 (d, J = 1.95 Hz, 5H), 7.29–7.34 (m, 2H), 6.85–6.91 (m, 1H), 5.21 (s, 2H), 5.06 (s, 2H), 3.72 (s, 3H); ES + MS: m/z = 399 (M+1).

A suspension of methyl 2-{[({[4-(methyloxy)phenyl]methyl} amino)carbonyl][(phenylmethyl)oxy]amino}-3-pyridinecarboxylate (0.71 g, 1.83 mmol) in Acetonitrile (16 mL)/Water (1.6 mL) was treated with cerium (IV) ammonium nitrate (5.0 g, 9.13 mmol) and heated to reflux. After 30 min, the reaction mixture was cooled, diluted with water and extracted with ethyl acetate. The combined organic layers were washed with $NaHCO_3$, brine, dried ($MgSO_4$), filtered and concentrated. The residue was purified by silica gel chromatography (0–10% MeOH/dichloromethane) to afford the title compound (0.39 g, 1.4 mmol, 79% yield) as a yellow solid: ^{1}H NMR (400 MHz, DMSO-d_6) δ ppm 11.92 (s, 1H), 8.79 (dd, J = 1.7, 4.9 Hz, 1H), 8.35 (dd, J = 1.7, 7.8 Hz, 1H), 7.62 (dd, J = 1.6, 7.6 Hz, 2H), 7.47–7.36 (m, 5H), 5.17 (s, 2H); ES + MS: m/z = 270 (M+1).

*4.1.1.5. 4-Chloro-1-[(phenylmethyl)oxy]pyrido[2,3-d]pyrimidin-2(1H)-one (**14**).* A solution of 1-[(phenylmethyl)oxy]pyrido[2,3-d] pyrimidine-2,4(1H, 3H)-dione (60 mg, 0.223 mmol) in diisopropylethylamine (195 μL, 1.114 mmol) was treated with phosphorus(V)oxychloride (104 μL, 1.114 mmol) and heated to 100 °C. After 45 min, the reaction mixture was concentrated *in vacuo* and the residue (62 mg, 97%) was used immediately without further purification: ^{1}H NMR (400 MHz, DMSO-d_6) δ ppm 9.00 (dd, J = 4.62, 1.61 Hz, 1H), 8.50 (dd, J = 7.95, 1.72 Hz, 1H) 7.66 (dd, J = 7.52, 1.72 Hz, 2H), 7.56 (dd, J = 8.17, 4.73 Hz, 1H), 7.42–7.46 (m, 3H), 5.22 (s, 2H); ES + MS: m/z = 288 (M+1).

*4.1.1.6. 1-(Benzyloxy)-4-((4-fluorobenzyl)amino)pyrido[2,3-d]pyrimidin-2(1H)-one (**16**).* A solution of 4-chloro-1-[(phenylmethyl) oxy]pyrido[2,3-d]pyrimidin-2(1H)-one (40 mg, 0.139 mmol) in DMF (1.4 mL) was treated with [(4-fluorophenyl)methyl]amine (174 mg, 1.390 mmol) and stirred at ambient temperature. After 2 h, the reaction mixture was concentrated *in vacuo* and purified by reverse phase HPLC to afford the title compound (32 mg, 61.2%) as a white solid: ES + MS: m/z = 377 (M+1).

*4.1.1.7. 4-{[(4-Fluorophenyl)methyl]amino}-1-hydroxypyrido[2,3-d] pyrimidin-2(1H)-one hydrobromide (**18**).* A solution of 4-{[(4-fluorophenyl)methyl]amino}-1-[(phenylmethyl)oxy]pyrido[2,3-d] pyrimidin-2(1H)-one (41 mg, 0.109 mmol) in acetic acid (1.3 mL) was treated with HBr (179 μL, 1.089 mmol, 33% in acetic acid), and warmed to 80 °C. After 6 h, the reaction mixture was concentrated *in vacuo* and purified by reverse phase HPLC to afford the title compound as a white solid (34 mg, 85%): ^{1}H NMR (400 MHz, DMSO-d_6) δ ppm 10.37 (s, 1H), 9.05 (s, 1H), 8.69 (dd, J = 1.5, 4.8 Hz, 1H), 8.54 (dd, J = 1.5, 8.0 Hz, 1H), 7.41 (dd, J = 5.6, 8.4 Hz, 2H), 7.28 (dd, J = 4.8, 8.0 Hz, 1H), 7.17 (t, J = 8.9 Hz, 2H), 4.68 (d, J = 5.5 Hz, 2H); ES + MS: m/z = 287 (M+1).

4.1.2. Procedure B (O^tBu protecting group)

4.1.2.1. 2-(tert-Butoxyamino)nicotinonitrile. A mixture of 3-cyano-2-fluoropyridine (9.0 g, 73.71 mmol), *O-tert*-butyl hydroxylamine hydrochloride (10.17 g, 81.0 mmol) and DIPEA (28.32 mL, 162.3 mmol) was heated in a microwave at 120 °C. After 9 h, the reaction mixture was cooled to ambient temperature and partitioned between EtOAc and water. The organics were washed with brine, and the aqueous layer was extracted 3× with EtOAc. The organic phases were combined, dried (Na_2SO_4), and concentrated *in vacuo* to provide crude 2-(*tert*-butoxyamino)nicotinonitrile (13.11 g, 93% yield) as dark red oil which solidified upon standing. ^{1}H NMR (400 MHz, $CDCl_3$) δ ppm 8.34 (dd, J = 1.6, 5.2 Hz, 1H), 8.82 (dd, J = 1.6, 7.6 Hz, 1H), 7.44 (s, 1H), 6.85 (dd, J = 5.2, 7.6 Hz, 1H), 1.39 (s, 9H); ES + MS: m/z = 192.3 (M+1).

4.1.2.2. 2-(tert-Butoxyamino)-3-pyridinecarboxylic acid. To a solution of 2-(*tert*-butoxyamino)nicotinonitrile (9.00 g, 47.1 mmol) in methanol was added a solution of NaOH (8.69 g, 141.0 mmol) in water (50.0 mL), and the mixture was heated at 100 °C. After 13 h, the reaction mixture was cooled to ambient temperature and acidified to pH = 3–4 with 1 M HCl. The mixture was concentrated *in vacuo* and subsequently azeotroped with acetonitrile 3×. The residue was purified by silica gel chromatography (0–20% MeOH in DCM) to afford 2-(*tert*-butoxyamino)-3-pyridinecarboxylic acid (8.76 g, 79% yield) as a yellow solid: ^{1}H NMR (400 MHz, $CDCl_3$) δ ppm 8.50 (d, J = 6.8 Hz, 1H), 8.32 (d, J = 6.8 Hz, 1H), 6.72 (t, J = 6.8 Hz, 1H), 1.41 (s, 9H); ES + MS: m/z = 211.2 (M+1).

*4.1.2.3. Methyl 2-(tert-butoxyamino)-3-pyridinecarboxylate (**11**).* A solution of 2-(*tert*-butoxyamino)-3-pyridinecarboxylic acid (4.06 g, 19.31 mmol) in diethyl ether (54.6 mL) and methanol (54.6 mL), was treated with TMS-diazomethane (2 M in hexanes) (19.31 mL, 38.62 mmol) dropwise. After 5 min, excess TMS-diazomethane was quenched by the dropwise addition of AcOH until gas evolution ceased. The reaction mixture was concentrated *in vacuo* and the residue was purified by silica gel chromatography (25% EtOAc in hexanes) to afford methyl 2-(*tert*-butoxyamino)-3-pyridinecarboxylate (4.18 g, 97% yield) as yellow oil: ^{1}H NMR (400 MHz, $CDCl_3$) δ ppm 9.85 (s, 1H), 8.42 (dd, J = 2.0, 4.8 Hz, 1H), 8.13 (dd, J = 2.0, 7.6 Hz, 1H), 6.68 (dd, J = 4.8, 7.6 Hz, 1H), 3.87 (s, 3H), 1.34 (s, 9H); ES$^+$ MS: m/z = 225.3 (M+1).

*4.1.2.4. 1-(tert-Butoxy)pyrido[2,3-d]pyrimidine-2,4(1H, 3H)-dione (**13**).* A solution of methyl 2-(*tert*-butoxyamino)-3-pyridinecarboxylate (4.18 g, 18.64 mmol) in 1,2-dichloroethane (240 mL) was treated with trichloroacetyl isocyanate (4.93 mL, 41.6 mmol) dropwise. After 2 h, the reaction mixture was concentrated *in vacuo* and treated with methanol (240 mL) and sodium methoxide (20.14 mL, 93 mmol) (25% by weight in MeOH). After 45 min, the reaction mixture was concentrated *in vacuo* and was treated with 1 N HCl (42 mL) and the 0.1 N HCl (85 mL). The layers were partitioned and the organic phase was washed with brine, dried over Na_2SO_4, filtered and concentrated. The residue was purified by silica gel chromatography (0–30% EtOAc in hexanes) to afford 1-(*tert*-butoxy)pyrido[2,3-d]pyrimidine-2,4(1H, 3H)-dione (3.27 g, 74.6% yield) as a light yellow solid: ^{1}H NMR (400 MHz, $CDCl_3$) δ ppm 9.29 (s, 1H), 8.71 (dd, J = 2.0, 4.8 Hz, 1H), 8.44 (dd, J = 2.0, 7.6 Hz, 1H), 7.25 (dd, J = 4.8, 7.6 Hz, 1H), 1.48 (s, 9H); ES$^+$ MS: m/z = 236.4 (M+1).

*4.1.2.5. 4-(4,4-Difluoro-1-piperidinyl)-1-[(1,1-dimethylethyl)oxy]pyrido[2,3-d]pyrimidin-2(1H)-one (**17**).* A solution of 1-(*tert*-butoxy) pyrido[2,3-d]pyrimidine-2,4(1H, 3H)-dione (42 mg, 0.177 mmol) in toluene (3 mL) was treated with DIPEA (0.16 mL, 0.89 mmol) and $POCl_3$ (0.04 mL, 0.44 mmol) and the mixture was heated at 100 °C. After 1 h, the solvent was removed *in vacuo* to afford 4-chloro-1-(*tert*-butoxy)pyrido[2,3-d]pyrimidin-2(1H)-one (15) that was used immediately without further purification.

A solution of 4-chloro-1-(*tert*-butoxy)pyrido[2,3-d]pyrimidin-2(1H)-one (45 mg, 0.177 mmol) in N,N-dimethylformamide (5 mL) and DIPEA (2.0 mL, 11.45 mmol) was treated with 4,4-difluoropiperidine (335 mg, 2.129 mmol) and stirred at ambient temperature. After 15 min, the mixture was diluted by EtOAc, and washed with water and brine, dried over Na_2SO_4 and concentrated *in vacuo*. The residue was purified by silica gel chromatography (0–5% MeOH in DCM) to provide 4-(4,4-difluoro-1-piperidinyl)-1-

[(1,1-dimethylethyl)oxy]pyrido[2,3-d]pyrimidin-2(1H)-one (48.9 mg, 0.145 mmol, 81% yield) as a brown oil: ^{1}H NMR (400 MHz, $CDCl_3$) δ ppm 8.60 (d, J = 4.8 Hz, 1H), 7.85 (d, J = 8.0 Hz, 1H), 7.10 (dd, J = 4.8, 8.0 Hz, 1H), 8.88 (m, 4H), 2.12 (m, 4H), 1.42 (s, 9H); ES$^+$ MS: m/z = 339.4 (M+1).

*4.1.2.6. 4-(4,4-Difluoropiperidin-1-yl)-1-hydroxypyrido[2,3-d]pyrimidin-2(1H)-one (**19**).* A solution of 4-(4,4-difluoro-1-piperidinyl)-1-(*tert*-butoxy)pyrido[2,3-d]pyrimidin-2(1H)-one (48.9 mg, 0.145 mmol) in dichloromethane (10 mL), was treated with trifluoroacetic acid (1.0 mL). After 4 h, the reaction mixture was concentrated *in vacuo*. The residue was crystallized from MeOH/DCM to afford 4-(4,4-difluoro-1-piperidinyl)-1-hydroxypyrido[2,3-d]pyrimidin-2(1H)-one (37.8 mg, 65.3% yield) as a brown solid: ^{1}H NMR (400 MHz, METHANOL-d4) δ ppm 8.70 (dd, J = 1.6, 4.7 Hz, 1H), 8.34 (s, 1H), 7.37–7.30 (m, 1H), 4.01–3.91 (m, 4H), 2.19 (s, 4H); ES$^+$ MS: m/z = 282.9 (M+1).

*4.1.2.7. 4-((Cyclopropylmethyl)amino)-1-hydroxypyrido[2,3-d]pyrimidin-2(1H)-one (**20**).* The title compound was prepared using procedure A to provide a white solid (6.12 mg, 90%) as a TFA salt. ^{1}H NMR (400 MHz, DMSO-d_6) δ ppm 8.73 (br. s., 1H), 8.67 (dd, J = 1.5, 4.7 Hz, 1H), 8.55 (dd, J = 1.5, 8.0 Hz, 1H), 7.27 (dd, J = 4.7, 8.0 Hz, 1H), 3.36–3.27 (m, 2H), 1.13 (d, J = 17.3 Hz, 1H), 0.52–0.43 (m, 2H), 0.33–0.24 (m, 2H); ES + MS: 233 (M+1).

*4.1.2.8. 4-([1,1′-Biphenyl]-4-ylamino)-1-hydroxypyrido[2,3-d]pyrimidin-2(1H)-one (**21**).* The title compound was prepared using procedure A to provide the title compound as a TFA salt following purification by reverse phase HPLC: ^{1}H NMR (400 MHz, DMSO-d_6) δ ppm 10.05–9.94 (m, 1H), 8.85–8.72 (m, 2H), 7.94 (d, J = 8.4 Hz, 2H), 7.72 (dd, J = 8.2, 10.9 Hz, 4H), 7.48 (t, J = 7.7 Hz, 2H), 7.41–7.32 (m, 2H); ES + MS: 331 (M+1).

*4.1.2.9. 4-(([1,1′-Biphenyl]-4-ylmethyl)amino)-1-hydroxypyrido[2,3-d]pyrimidin-2(1H)-one (**22**).* The title compound was prepared using a procedure B to provide the title compound as a TFA salt: ^{1}H NMR (400 MHz, DMSO-d_6) δ ppm 10.21–10.09 (m, 1H), 8.90 (d, J = 6.6 Hz, 2H), 8.84 (d, J = 8.1 Hz, 1H), 8.78 (dd, J = 1.4, 4.6 Hz, 1H), 8.33 (d, J = 6.6 Hz, 2H), 8.18–8.10 (m, 4H), 7.40 (dd, J = 4.7, 8.1 Hz, 1H); ES$^+$ MS: 344.9 (M+1).

*4.1.2.10. 1-Hydroxy-4-((4-(pyridin-4-yl)phenyl)amino)pyrido[2,3-d]pyrimidin-2(1H)-one (**23**).* The title compound was prepared using procedure A to provide the title compound as a TFA salt: ^{1}H NMR (300 MHz, DMSO-d_6) δ ppm 10.16 (s, 1H), 8.87 (m, 4H), 8.35 (m, 2H), 8.15 (m, 4H), 7.41 (m, 1H), 3.17 (s, 1H); ES$^+$ MS: 332 (M+1).

*4.1.2.11. 1-Hydroxy-4-({[4-(4-pyridinyl)phenyl]methyl}amino)pyrido[2,3-d]pyrimidin-2(1H)-one (**24**).* The title compound was prepared using procedure B to provide the title compound as a TFA salt: ^{1}H NMR (300 MHz, DMSO-d_6) δ ppm 9.17 (m, 1H), 8.80 (m, 1H), 8.70 (d, 1H), 8.57 (d, 1H), 8.07 (d, 2H), 7.91 (d, 2H), 7.56 (d, 2H), 7.30 (m, 1H), 4.78 (d, 2H); ES$^+$ MS: 346.0 (M+1).

*4.1.2.12. 1-Hydroxy-4-{[4-(4-morpholinyl)phenyl]amino}pyrido[2,3-d]pyrimidin-2(1H)-one (**25**).* The title compound was prepared using procedure B to provide the title compound as a TFA salt following purification by reverse phase HPLC: ^{1}H NMR (400 MHz, DMSO-d_6) δ ppm 9.81 (s, 1H), 8.80–8.66 (m, 2H), 7.63 (d, J = 8.9 Hz, 2H), 7.32 (dd, J = 4.7, 8.0 Hz, 1H), 6.99 (d, J = 9.1 Hz, 2H), 3.82–3.71 (m, 4H), 3.16–3.06 (m, 4H); ES$^+$ MS: 339.9 (M+1).

*4.1.2.13. 1-Hydroxy-4-({[4-(4-morpholinyl)phenyl]methyl}amino)pyrido[2,3-d]pyrimidin-2(1H)-one (**26**).* The title compound was prepared using procedure B to provide the title compound as a TFA salt: ^{1}H NMR (400 MHz, DMSO-d_6) δ ppm 9.04 (s, 1H), 8.67 (dd, J = 1.5, 4.7 Hz, 1H), 8.55 (dd, J = 1.5, 8.0 Hz, 1H), 7.28–7.19 (m, 3H), 6.92 (d, J = 8.7 Hz, 2H), 4.60 (d, J = 5.5 Hz, 2H), 3.77–3.68 (m, 4H), 3.12–3.03 (m, 3H); ES$^+$ MS: 354.0 (M+1).

*4.1.2.14. 1-Hydroxy-4-((4-(morpholinomethyl)phenyl)amino)pyrido[2,3-d]pyrimidin-2(1H)-one (**27**).* The title compound was prepared using procedure B to provide the title compound as a TFA salt: ^{1}H NMR (300 MHz, DMSO-d_6) δ ppm 10.63 (s, 1H), 10.05 (s, 1H), 8.84–8.77 (m, 2H), 7.96 (d, 2H), 7.55 (s, 2H), 7.40 (dd, 1H), 4.37 (s, 2H), 4.01–3.98 (m, 2H), 3.69–3.61 (m, 2H), 3.40 (m, 2H), 3.29–3.18 (m, 2H); ES$^+$ MS: 354.1 (M+1).

*4.1.2.15. 1-Hydroxy-4-({[3-(4-morpholinyl)phenyl]methyl}amino)pyrido[2,3-d]pyrimidin-2(1H)-one (**28**).* The title compound was prepared using procedure B to provide the title compound as a TFA salt: 1H NMR (400 MHz, METHANOL-d4) Shift = 8.67 (d, J = 4.5 Hz, 1H), 8.51 (br. s., 1H), 7.49–7.17 (m, 5H), 4.76 (br. s., 2H), 3.92 (br. s., 4H), 3.41 (br. s., 4H); ES$^+$ MS: 354.0 (M+1).

*4.1.2.16. 1-Hydroxy-4-({[3-(4-morpholinylmethyl)phenyl]methyl}amino)pyrido[2,3-d]pyrimidin-2(1H)-one (**29**).* The title compound was prepared using procedure A to provide the title compound as a TFA salt following purification by reverse phase HPLC: 1H NMR (400 MHz, METHANOL-d4) Shift = 8.65 (d, J = 4.6 Hz, 1H), 8.45 (d, J = 7.2 Hz, 1H), 7.62 (br. s., 1H), 7.52–7.24 (m, 4H), 4.74 (s, 2H), 4.32 (br. s., 2H), 4.05–3.94 (m, 2H), 3.68 (t, J = 11.5 Hz, 2H), 3.31 (s, 2H), 3.15 (d, J = 9.6 Hz, 2H); ES + MS: 368 (M+1).

4.2. Virology

4.2.1. Reagents

Reverse transcriptase and integrase were prepared as previously described [21]. Deoxynucleotide triphosphates (dNTPs) and protease-free Bovine Serum Albumin (BSA; Fraction V) were acquired from Roche Applied Science (Indianapolis, IN). [8-^{3}H(N)]-deoxyguanosine 5′-triphosphate (dGTP) and streptavidin-coated polystyrene SPA imaging beads were acquired from PerkinElmer (Waltham, MA). 1,4-dithiothreitol (DTT), CHAPS and dimethyl sulfoxide (DMSO) were acquired from Sigma–Aldrich (St. Louis, MO). NP-40 was acquired from Thermo Scientific (Rockford, IL). Nuclease-free dH_2O, Tris pH 8.0, NaCl, KCl, MgCl, and EDTA were acquired from Life Technologies (Grand Island, NY). All compounds were prepared as 10 mM stocks in DMSO and stored at −20 °C.

The following oligonucleotides were used and were acquired from Midland Certified Reagent Company (Midland, TX) and Integrated DNA Technologies (Coralville, IA).

Oligo 1, 5′-AGGUG AGUGA GAUGA UAACA AAUUU GCGAG CCCCA GAUGC-3′

Oligo 2, 5′-Biotin-GCATC TGGGG CTCGC AAATT TG-3′

Oligo 3, 5′-CCCCC CCCCC CCCCC AGGTG AGTGA GATGA TAAC-cordycepin-3′

All lyophilized oligonucleotides were reconstituted to 200 μM in 10 mM Tris pH 8.0, 10 mM NaCl and stored at −20 °C in small aliquots prior to use.

Substrate A was prepared by equilibrating 20 μM of Oligo 1 and 20 μM of Oligo 2 in 10 mM Tris pH 8.0, 10 mM NaCl at 95 °C, followed by a gradual decrease to 80 °C (0.1 °C decrease/6 s) and then to 4 °C (0.1C/20 s) with a Dyad DNA Engine thermal cycler (BioRad; Hercules, CA).

4.2.2. Reverse transcriptase RNase H strand transfer activity

Test compounds were serially diluted in DMSO and plated (0.1 μL) in low volume, white 384-well plates. High and low

control wells contained 0.1 μL of DMSO alone. To start the assay, 5 μL of 2× enzyme solution (40 nM RT in assay buffer (50 mM Tris pH 8.0, 80 mM KCl, 10 mM $MgCl_2$, 0.02% NP-40, 5 mM DTT, Nuclease-free dH_2O)) were dispensed to all but the low control wells, which received 5 μL of assay buffer only, and the enzyme was allowed to incubate with the test compounds for 30 min at room temperature. The assay was initiated by the addition of 5 μL of 2× substrate (400 nM dATP, 400 nM dCTP, 400 nM dTTP, 54 nM [8-^{3}H(N)]-dGTP, 20 nM Substrate A, and 200 nM Oligo 3 in assay buffer) to each well. The final assay composition was 50 mM Tris pH 8.0, 80 mM KCl, 10 mM $MgCl_2$, 0.02% NP-40, 5 mM DTT, 200 nM dATP, 200 nM dCTP, 200 nM dTTP, 27 nM [8-^{3}H(N)]-dGTP, 10 nM Substrate A, 100 nM Oligo 3, 20 nM RT, and 0.169 nM–10 μM test compound.

After incubating for 90 min, the reaction was stopped via the addition of 10 μL of quench buffer (50 mM Tris pH 8.0, 80 mM KCl, 50 mM EDTA, 50 μM CHAPS, 0.1 mg/mL BSA, and 0.3 mg/mL streptavidin-coated polystyrene SPA imaging beads) to all wells. Plates were read with a ViewLux (Perkin–Elmer; Waltham, MA) after overnight incubation at room temperature.

The data for dose responses were plotted as % Inhibition versus compound concentration following normalization using the formula 100*((U − C1)/(C2 − C1)), where U was the unknown value, C1 was the average of the high (0% Inhibition) control wells and C2 was the average of the low (100% Inhibition) control wells. Curve fitting was performed with the equation $y = A + ((B - A)/(1 + (10^x/10^C)^D))$, where A was the minimum response, B was the maximum response, C was the log (XC_{50}) and D was the Hill slope. The results for each test compound were recorded as pIC_{50} values (−C in the above equation).

4.2.3. Integrase strand transfer assay

Performed as previously described [22].

4.3. In vivo DMPK

Male non fasted Sprague Dawley (CD) rats ($n = 2$ per study arm) received test article at doses of 1 mg/kg i.v. (1 mL/kg) or 5 mg/kg p.o. (5 mL/kg), formulated in a 10% DMSO/10% Solutol/80% 0.05 M N-methylglucamine dosing vehicle. For all animals, water was provided *ad libitum*. Blood samples were withdrawn from a surgically-implanted venous cannula at timed intervals for 24 h after dose administration, treated with EDTA, and centrifuged to harvest plasma for LC/MS/MS analysis. Plasma concentration–time data for individual rats were analyzed using non compartmental analysis (WinNonlin v. 4.1a; Pharsight, Mountain View CA) to generate pharmacokinetic parameter estimates.

Acknowledgments

The authors would like to acknowledge the contributions of Derek Parks, Iris Paulus, and Rob Ferris.

Appendix A. Supplementary data

Supplementary data related to this article can be found at http://dx.doi.org/10.1016/j.ejmech.2014.06.061.

References

[1] M. Andreola, Curr. Pharm. Des. 10 (2004) 3713–3723.
[2] S. Gabbara, W. Davis, L. Hipe, D. Hupe, J. Peliska, Biochemistry 38 (1999) 13070–13076.
[3] J.H. Chan, G.A. Freeman, J. Tidwell, K. Romines, L. Schaller, J.R. Cowan, S.S. Gonzales, G.S. Lowell, C.W. Andrews III, D.J. Reynolds, M. St Clair, R.J. Hazen, R.G. Ferris, K.L. Creech, G.B. Roberts, S.A. Short, K. Weaver, G.W. Koszalka, L.R. Boone, J. Med. Chem. 47 (2004) 1175–1182.
[4] A. Parniak, K.L. Min, S.R. Budihas, S.F. Le Grice, J.A. Beutler, Anal. Biochem. 322 (2003) 33–39.
[5] S. Hare, S.S. Gupta, E. Valkov, A. Engelman, P. Cherepanov, Nature 464 (2010) 232–236.
[6] S. Hare, A.M. Vos, R.F. Clayton, J.W. Thuring, M.D. Cummings, P. Cherepanov, Proc. Natl. Acad. Sci. U. S. A. 107 (2010) 20057–20062.
[7] T.A. Kirschberg, M. Balakrishnan, N.H. Squires, T. Barnes, K.M. Brendza, X. Chen, E.J. Eisenberg, W. Jin, N. Kutty, S. Leavitt, A. Liclican, Q. Liu, X. Liu, J. Mak, J.K. Perry, M. Wang, W.J. Watkins, E.B. Lansdon, J. Med. Chem. 52 (2009) 5781–5784.
[8] D.M. Himmel, K.A. Maegley, T.A. Pauly, J.D. Bauman, K. Das, C. Dharia, A. Clark, K. Ryan, M.J. Hickley, R.A. Love, S.J. Hughes, S. Bergqvist, E. Arnold, Structure 17 (2009) 1625–1635.
[9] A. Pendri, N.A. Meanwell, K.M. Peese, M.A. Walker, Expert Opin. Ther. Pat. 21 (2011) 1173–1189.
[10] S. Hare, S.J. Smith, M. Metifiot, A.J. Chamiec, Y. Pommier, S.H. Hughes, P. Cherepanov, Mol. Pharmacol. 80 (2011) 565–572.
[11] D.J. Hazuda, N.J. Anthony, R.P. Gomez, S.M. Jolly, J.S. Wai, L. Zhuang, T.E. Fisher, M. Embrey, J.P. Guare, M.S. Egbertson, J.P. Vacca, J.R. Huff, P.J. Felock, M.V. Witmer, K.A. Stillmock, R. Danovich, J. Grobler, M.D. Miller, A.S. Espeseth, L. Jin, I. Chen, J.H. Lin, K. Kassahun, J.D. Ellis, B.K. Wong, W. Xu, P.G. Pearson, W.A. Schleif, R. Cortese, E. Emini, V. Summa, M.K. Holloway, S.D. Young, Proc. Natl. Acad. Sci. U. S. A. 101 (2004) 11233–11238.
[12] K. Klumpp, J.Q. Hang, S. Rajendran, Y. Yang, A. Deosier, P.W.K. In, H. Overton, K.E.B. Parkes, N. Cammack, J.A. Martin, Nucl. Acids Res. 31 (2003) 6852–6859.
[13] T. Kawasuji, B.A. Johns, H. Yoshida, T. Taishi, Y. Taoda, H. Murai, R. Kiyama, M. Fuji, T. Yoshinaga, T. Seki, M. Kobayashi, A. Sato, T. Fujiwara, J. Med. Chem. 55 (2012) 8735–8744.
[14] P.D. Williams, D.D. Staas, S. Venkatraman, H.M. Loughran, R.D. Ruzek, T.M. Booth, T.A. Lyle, J.S. Wai, J.P. Vacca, B.P. Feuston, L.T. Ecto, J.A. Flynn, D.J. DiStefano, D.J. Hazuda, C.M. Bahnck, A.L. Himmelberger, G. Dornadula, R.C. Hrin, K.A. Stillmock, M.V. Witmer, M.D. Miller, J.A. Grobler, Bioorg. Med. Chem. Lett. 20 (2010) 6754–6757.
[15] H.P. Su, Y. Yu, G.S. Prasad, R.F. Smith, C.L. Daniels, P.D. Abeywickrema, J.C. Reid, H.M. Loughran, M. Kornienko, S. Sharma, J.A. Grobler, B. Xu, V. Sardana, T.J. Allison, P.D. Williams, P.L. Darke, D.J. Hazuda, S. Munshi, J. Virol. 84 (2010) 7625–7633.
[16] E.P. Garvey, B.A. Johns, M.J. Gartland, S.A. Foster, W.H. Miller, R.G. Ferris, R.J. Hazen, M.R. Underwood, E.E. Boros, J.B. Thompson, J.G. Weatherhead, C.S. Koble, S.H. Allen, L.T. Schaller, R.G. Sherrill, T. Yoshinaga, M. Kobayashi, C. Wakasa-Morimoto, S. Miki, K. Nakahara, T. Noshi, A. Sato, T. Fujiwara, Antimicrob. Agents Chemother. 52 (2008) 901–908.
[17] T.J. Ritchie, S.J. Macdonald, Drug Discov. Today 14 (2009) 1011–1020.
[18] J.D. Hughes, J. Blagg, D.A. Price, S. Bailey, G. DeCrescenzo, R.V. Devraj, E. Ellsworth, Y.M. Fobian, M.E. Gibbs, R.W. Gilles, N. Greene, E. Huang, T.K. Burke, J. Loesel, T. Wagner, L. Whiteley, Y. Zhang, Bioorg. Med. Chem. Lett. 18 (2008) 4872–4875.
[19] R.J. Young, D.V. Green, C.N. Luscombe, A.P. Hill, Drug Discov. Today 16 (2011) 822–830.
[20] R.J. Young, Bioorg. Med. Chem. Lett. 21 (2011) 6228–6235.
[21] E.P. Garvey, B. Schwartz, M.J. Gartland, S. Lang, W. Halsey, G. Sathe, H.L. Carter III, K.L. Weaver, Biochemistry 48 (2009) 1644–1653.
[22] E.E. Boros, B.A. Johns, E.P. Garvey, C.S. Koble, W.H. Miller, Bioorg. Med. Chem. Lett. 16 (2006) 5668–5672.